Tellus (1997), 49A, 474–485
Printed in UK – all rights reserved

TELLUS
ISSN 0280–6495

Scaling laws for barotropic vortex beta-drift

By RONALD B. SMITH*, *Department of Geology and Geophysics, Yale University, New Haven, Connecticut, 06511, USA*; XIAOFAN LI and BIN WANG, *Department of Meteorology, University of Hawaii at Manoa, Honolulu, Hawaii, 96822, USA*

(Manuscript received 10 July 1996; in final form 11 March 1997)

ABSTRACT

A steady-state formulation of dimensional analysis is used to consolidate vortex beta drift data from over 100 single-layer numerical simulations. The physical problem of beta drift considered here includes 5 parameters: vortex radius, vortex maximum wind, beta, a dimensionless vortex profile exponent and the strength of the meridional shear of the zonal environmental wind. The use of dimensional analysis reduces these 5 parameters to 3, and the further use of the square root scaling proposed by Smith reduces the problem to 2 parameters, the vortex exponent b and a shear parameter S. The non-dimensional speed and direction of beta drift are given by $\hat{V}=C(b,S)B^{-1/2}$ and $\theta_d=D(b,S)$, where the functions $C(b,S)$ and $D(b,S)$ are determined empirically. The quantity B is a non-dimensional beta parameter. The proportionality between drift velocity and the square root of beta arises because the magnitude of the beta gyre vorticity is proportional to the square root of beta. An application of an empirical barotropic drift law to ensemble hurricane track forecasting is proposed.

1. Introduction

The influence of the beta effect on the poleward drift of hurricanes has been intensely studied over the past few years. In many of these investigations, the complicated dynamics of real hurricanes has been approximated by an inviscid, single-layer, non-divergent model of vorticity dynamics governed by

$$\frac{\partial \xi}{\partial t}+\mathbf{V}\cdot\nabla\xi+\beta v=0, \qquad (1)$$

where ξ is the vorticity and β is the meridional gradient in the planetary vorticity f (i.e., $\beta=df/dy$). Chan and Williams (1989) and others have shown that in such a simplified model, northwestward drift (in the northern hemisphere) occurs due to the advective effect of two "beta-gyres" which form northeast and southwest of the primary vortex. These two gyres of opposite sign are maintained by a balance of three terms in (1): the advection of planetary vorticity generating negative and positive anomolies east and west of the primary vortex, the counter clockwise rotation of these anomolies by the primary vortex and, the cancelling of the anomolies by the drift of the primary vortex. Until now, theoretical analysis of (1) has failed to yield either a concise formula for the steady state drift speed (V_d) and direction (θ_d) or a clear idea of the scaling laws. Recently, Smith (1993) applied the principle of dimensional analysis to the numerical results of Chan and Williams (1989) to determine an empirical beta-drift law.

$$\hat{V}(B)=0.9B^{-1/2}, \qquad (2)$$

where $B=\beta r_m^2/V_m$ and $\hat{V}=V_d/r_m^2\beta$. The two non-dimensional parameters B and $\hat{V}$, are defined in terms of the dimensional parameters which characterize the beta-drift problem: the value of beta (β), the maximum wind in the vortex (V_m), and the radius at which the maximum wind occurs (r_m).

* Corresponding author.

Eq. (2) implies that the drift speed $V_d \sim r_m\sqrt{V_m\beta}$. The drift law (2) is appropriate only for the particular vortex profile used by Chan and Williams, and valid only in the absence of environmental shear and other complicating factors. Smith (1993) also reported on a weak dependence of the drift angle θ_d on the nondimensional beta parameter B.

In this paper, we attempt to generalize (2) to include the influences of variable vortex profile and meridional shear in the zonal environmental wind. The strong influence of the vortex profile has been shown by DeMaria (1985) and the influence of shear has been shown recently by Williams and Chan (1994) and Wang and Li (1995). If a concise dimensionally-consistent closed-form drift law could be found which includes these effects, it would consolidate and quantify these previous works. More significantly, it would reveal how the physical factors which control beta-drift interact. This type of scale analysis has been shown to be an essential method in theoretical fluid dynamics; especially in non-linear problems for which no analytical solutions have yet been found.

The physical problem of beta-drift that we consider here has 5 parameters; the maximum tangential wind speed in the vortex "V_m", the radius at which that speed occurs "r_m", the value of beta $\beta = df/dy$, the shear in the zonal environmental wind $\alpha = dU/dy$, and a non-dimensional exponent related to the decrease of wind speed with radius in the outer part of the vortex b (see Section 3). To reduce the number of parameters from five to three we introduce the following definitions.

$$\bar{V} = r_m^2\beta \tag{3}$$

is a characteristic drift speed,

$$B = \beta r_m^2/V_m \tag{4}$$

is a non-dimensional beta parameter and

$$S = \alpha r_m/V_m \tag{5}$$

is a non-dimensional shear parameter. Using (3), the computed speed of vortex beta drift (V_d) can be nondimensionalized to give

$$\hat{V} = V_d/\bar{V}.$$

The computed drift direction θ_d is already a nondimensional quantity. According to the principle of dimensional analysis, the nondimensional drift speed and direction can be written in terms of the nondimensional control parameters

$$\hat{V} = \hat{V}(B, S, b), \tag{6}$$

and

$$\theta_d = \theta_d(B, S, b). \tag{7}$$

Eqs. (6) and (7) will hold if steady state drift occurs, so that time does not enter the list of dimensional parameters.

To make efficient progress towards the determination of an empirical drift law, it is useful to reduce the dimension of parameter space from three to two. Our hopes for achieving this simplification depend on the robustness of the square root beta scaling (2) proposed by Smith (1993). If his scaling is valid for variable vortex profile (b) and shear (S), then the parameter space dimension reduces to two, i.e. (S, b).

Our strategy is as follows. In Section 3, we examine the case with no shear ($S = 0$) and investigate the validity of square root beta scaling for a wide range of vortex profiles. In Section 4, we fix the vortex profile ($b = 1$) and investigate the square root beta scaling for a range of shear values. Finding that the "root beta" scaling is robust, we proceed in Section 5 to derive a general empirical drift law.

In Section 6, we discuss the physical significance of the root beta scaling. In Section 7, we propose an ensemble scheme for hurricane track forecasting using the empirical drift law derived herein.

2. Numerical simulations

The numerical model used in these experiments is a shallow water model used previously by Wang and Li (1992). The fast gravity wave speed in this model makes it behave in a nearly non-divergent way, approaching the dynamics given by (1). Because of this property, the constant f_0 in the beta plane formula $f(y) = f_0 + \beta y$ does not play a significant rôle. A discussion of the influence of divergence on beta drift is given by Grimshaw et al. (1994).

Each run was initialized with a symmetric balanced vortex (8) described in Section 3. The transient behavior of a vortex on a beta-plane is

composed of several phases: an acceleration phase, slowly decaying track oscillations, a "steady state" period and a Rossby wave dispersion period. Dimensional analysis suggests that three time scales govern this transient behavior: $T_1 = r_m/V_m$, $T_2 = (\beta V_m)^{-1/2}$ and $T_3 = 1/\beta r_m$. With parameters $r_m = 1000$ km, $V_m = 30$ m/s and $\beta = 1 \times 10^{-11} m^{-1} s^{-1}$, these time scales are $T_1 = 0.93$ hours, $T_2 = 16$ and $T_3 = 278$ h.

Our experiments indicate that for the same vortex, the value of beta controls both the length of the acceleration phase and the onset of dispersion, suggesting that T_2 and T_3 must be considered in defining the period of steady state drift. Accordingly, we examined a range of times "t" given by $T_2 \ll t \ll T_3$ in our search for steady state behaviour.

In no case was a perfect steady state achieved. Even after the acceleration phase was completed, the vortex drift vector continued to oscillate to some degree (see also Section 6). In this paper we have assumed that a steady state drift could exist, in principle, and we have tried to determine its properties by averaging over a period of noisy oscillating quasi-steady drift. An averaging period from 31 to 66 h was used for most runs, but for the smaller values of beta and larger values of b, steady state drift takes longer to develop and averaging a period from 61 to 72 h was used. In extreme cases, an even longer run (up to 144 hours) was required to reach a rough steady state. As we will see, the steady state hypothesis is well supported by the internal consistency of our results and the good agreement with other workers, each using different averaging periods.

3. Vortex profiles

In this section, we examine the influence of vortex profile on beta drift in an unsheared environment. We consider a family of vortex profiles given by Wang and Li (1992), and shown in Fig. 1.

$$V(r) = V_m \frac{r}{r_m}\left[\exp\left\{\frac{1}{b}\left[1-\left(\frac{r}{r_m}\right)^b\right]\right\} - \frac{|r-r_m|}{R_0-r_m}\exp\left\{\frac{1}{b}\left[1-\left(\frac{R_0}{r_m}\right)^b\right]\right\}\right], \quad r \leqslant R_0$$

$$= 0, \qquad r > R_0 \tag{8}$$

This formula contains 4 free parameters V_m, r_m, b, R_0. We will restrict our consideration to cases

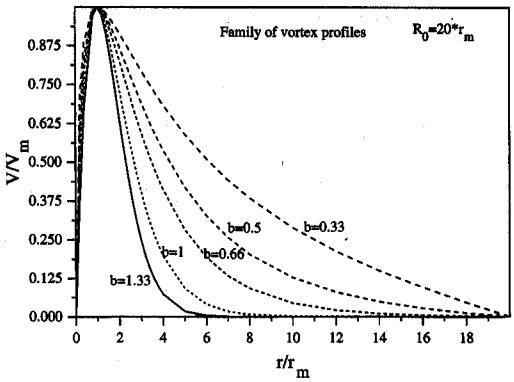

Fig. 1. The family of vortex profiles used in this investigation. The ratio of wind speed to the maximum wind speed (V_m) is plotted against the ratio of radius to the radius of maximum wind (r_m).

where R_0 is sufficiently greater than r_m so that (2) reduces approximately to:

$$V(r) = V_m \left(\frac{r}{r_m}\right) \exp\left(\frac{1}{b}\left(1-\left(\frac{r}{r_m}\right)^b\right)\right) \tag{9}$$

a profile used earlier by Chan and Williams (1989). Using an initial vortex given by (8) with $r_m = 50$ km, $V_m = 30$ m/s, $R_0 = 1000$ km, 24 numerical beta drift experiments were carried out. Four values of b were used: 0.33, 0.66, 1.0 or 1.33, and 6 values of beta (given by $\beta = 2^n \times 1.0725 \times 10^{-11} s^{-1} m^{-1}$, $n = 0, 1, 2, 3, 4, 5$).

The non-dimensional beta drift speeds for 24 runs with various β and b values are shown in Fig. 2. The drift speeds for $b = 1$ agree with the empirical law (2) derived from the numerical runs by Chan and Williams. In the Chan and Williams simulations, parameters r_m and V_m were varied with beta held constant. This agreement between the present results and those of Chan and Williams supports the use of the dimensional analysis to study beta drift and adds confidence to our numerical techniques and to the existence of a quasi steady state drift.

The second interesting aspect of Fig. 2 is that each data subset with constant b, fits a power law formula similar to (2) with a slope $= -\frac{1}{2}$, thus,

$$\hat{V} = g(b) B^{-1/2}. \tag{10}$$

The function $g(b)$ can be determined by plotting $g(b) \equiv \hat{V} B^{+1/2}$ versus b as is done in Fig. 3. A good

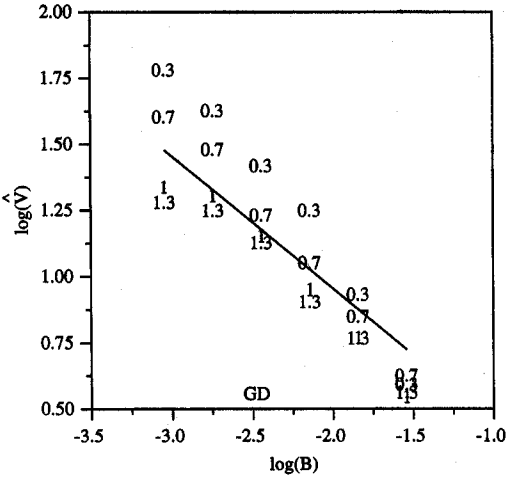

Fig. 2. The log (base ten) of the non-dimensional drift speed $\hat{V}$ versus the beta parameter B for four values of the vortex profile exponent $b=0.33$, 0.66, 1.0 and 1.33. The solid line is eq. (2). Letters D and G represent the B-values for hurricanes Dean and Gabrielle according to De Maria et al. (1992).

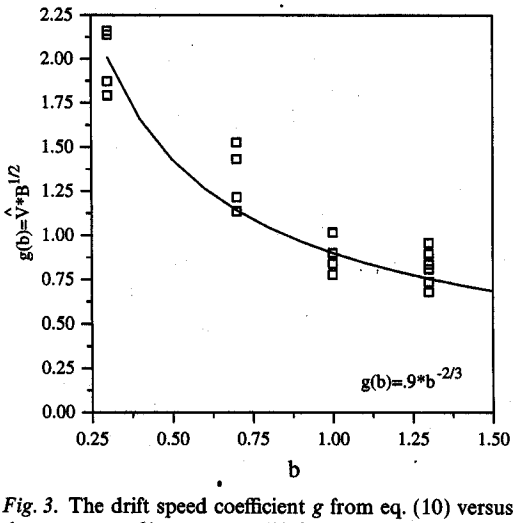

Fig. 3. The drift speed coefficient g from eq. (10) versus the vortex profile exponent (b) for runs with no shear. The solid line is eq. (11). Only data satisfying (12) is included.

fit to the data in Fig. 3 is given by

$$g(b) \equiv 0.9 b^{-2/3}. \qquad (11)$$

The coefficient (0.9) in (11) agrees with the coefficient (0.9) in (2). We have chosen to use approximate rational fractional exponents in (10) and (11) rather than more precise real values arising from a least-squares fit. This is done in part to emphasize that the numerical data itself is noisy and inaccurate and in part to make the formulae easier to remember and manipulate. The result (11) improves on the suggestion of Smith (1993) that $g(b) \sim b^{-1}$.

The third result revealed in Fig. 2 is that the power-law relationship (10) breaks down for larger values of B. Large values of B physically represent vortices with large radii and weak winds in a strong beta environment. Under these conditions, the vortex is distorted and it decays rapidly due to the radiation of Rossby waves. A true steady state is never achieved. In Fig. 2, it is apparent that vortices with small values of b (i.e., with a broad slowly decaying velocity profile), are more susceptible to this effect. With $b=0.33$, formula (10) breaks down for $\log B > -2.0$ while for $b=1.33$, (10) breaks down for $\log B > -1.6$. According to DeMaria et al. (1992), real hurricanes have rather broad velocity profiles with $b \approx 0.4$, suggesting that we should choose the more conservative validity range for (10)

$$\log B < -2.0 \quad \text{(i.e., } B < 0.01\text{)}, \qquad (12)$$

Even so, almost all real hurricanes satisfy (12).

The data from the 24 runs indicates that the direction of beta-drift depends on the value of b and is independent of the beta parameter B. As seen in Fig. 4, there is scatter in the drift angle

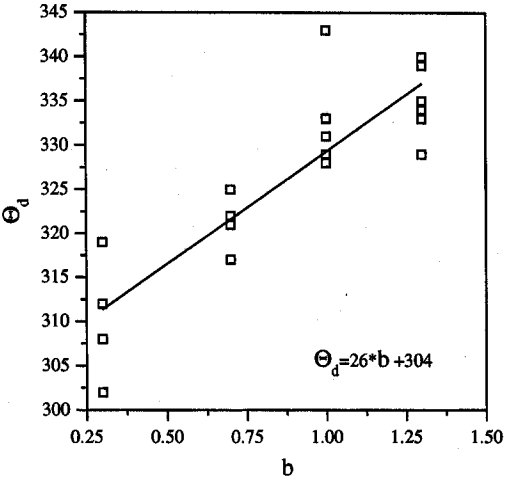

Fig. 4. The angle of beta drift (θ_d) is plotted against the vortex exponent b, for runs with no shear.

data of about $\pm 10°$. The relationship between θ_d and b is approximated by the linear formula:

$$\theta_d(b) = 304° + 26° \cdot b. \qquad (13)$$

Thus, a vortex with $b = 0.33$ drifts in the direction $\theta_d = 313° \pm 10°$, while a vortex with $b = 1.33$ has $\theta_d = 339° \pm 10°$. Note that θ_d is measured clockwise from true north.

The result that θ_d is independent of B is surprising as Smith's (1993) analysis of Chan and Williams (1987) results show an inverse relationship between these two variables. To verify our result, another 26 simulations were carried out to longer times (i.e., $t = 144$ h) and with slightly different parameters (i.e., $R_0/r_m = 10$). As before, uncertainties due to track oscillation and the identification of the steady state phase resulted in drift angle scatter, in this case $\pm 5°$, but no systematic dependence of θ_d on B could be seen. This discrepancy between Chan and Williams and our present result remains unexplained.

4. Meridional shear

It has recently been shown by Williams and Chan (1994) and Wang and Li (1995) that the beta-drift speed can be significantly modified if the zonal (i.e., E–W) wind in which the vortex is carried, has meridional (i.e., N–S) shear. Using a symmetry argument, in the case of constant shear, it is clear that shear cannot induce a drift by itself. Shear, acting on a vortex, produces an azimuthal wavenumber-two disturbance on the vortex and such a quadrupole pattern of vorticity induces no advective velocity at the vortex center. The shear can however, modify the wavenumber-one beta-gyres by aiding or resisting their advection by the cyclonic vortex winds.

In order to describe the effect of large-scale shear, we performed 30 hurricane drift simulations on a beta plane using the vortex profile (8) with $b = 1$. Four values for beta and seven values of meridional shear were used. The ratio of R_0/r_m in (8) was fixed at 7.5 so that the vortex was characterized by only two parameters, V_m and r_m. With $b = 1$, it is not necessary to set R_0/r_m as large as 20 in order to have (8) approximate (9). The zonal wind in the simulations was given by

$$U(y) = \alpha y, \qquad (14)$$

where α is the meridional shear. The non-dimensional shear parameter is $S = \alpha r_m / V_m$. If steady state vortex drift is achieved in the simulation, the principle of dimensional analysis requires that

$$\hat{V} = \hat{V}(B, S) \quad \text{only}. \qquad (15)$$

28 of the 30 calculations were done with standard values of $r_m = 100$ km and $V_m = 30$ m/s. In the other 2 runs, we altered these parameters and compared them with 2 standard runs to check (15). The results of these four runs are shown in Table 1. The agreement in the non-dimensional drift velocity between the pairs B5-B12 and B6-B11 is quite good, even though their dimensional values are quite different. These points appear in Fig. 5 at the far left and right labeled "2" to indicate their S value (i.e., $S = 0.0196$). The agreement adds confidence to our numerical procedures and to the existence of a quasi steady state drift.

The results from 30 runs are shown in Fig. 5, where non-dimensional drift speed is plotted against the non-dimensional beta parameter. The non-dimensional shear for each point is represented by an integer given approximately by $S \times 100$ (i.e., 0.0196 is represented as 2). The solid line in Fig. 5 is the "zero-shear" empirical law (2) from Smith (1993). The zero-shear empirical law agrees reasonably well with the zero-shear data points. This agreement was expected as Chan and Williams (1989), from whose data the law is derived, used a vortex profile (9) which is only slightly different than (8).

For non-zero shear, each set of points with equal shear forms a well defined line with a slope similar to that of the zero shear line. The constant slope indicates that even with shear, the $\hat{V} \sim B^{-1/2}$ behavior in (2) is still true. This proportionality suggests that the new drift law we seek may be of the form:

$$\hat{V} = f(S)\, B^{-1/2}. \qquad (16)$$

To determine the function f in (16) $f(S) = \hat{V} B^{+1/2}$ is plotted versus S in Fig. 6. In spite of considerable scatter, the function $f(S)$ is well defined and can be least-squares fit by a quadratic expression

$$f(S) = 154.2\, S^2 + 12.3S + 0.93, \qquad (17)$$

over the range of the data. The constant term in (17) agrees approximately with the coefficient in (2).

Table 1. *Four runs to check the scaling law in the presence of shear*

Run	β (10^{11} m^{-1} s^{-1})	r_m (km)	V_m (m/s)	α (10^5 s^{-1})	V_d (m/s)	B	S	$\hat{V}$
B5	1.075	100	30	0.5875	2.14	0.00358	0.0196	19.91
B6	4.290	100	30	0.5875	4.76	0.01430	0.0196	11.10
B11	2.145	200	60	0.5875	9.08	0.01430	0.0196	10.60
B12	2.145	50	15	0.5875	1.10	0.00358	0.0196	20.51

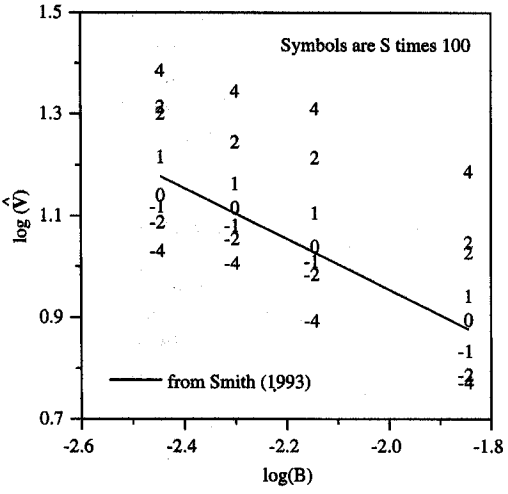

Fig. 5. The log (base ten) of the non-dimensional drift speed versus the beta parameter for different values of meridional shear. Symbols are the values of the non-dimensional meridional shear, given as an integer (i.e., $S \times 100$). The solid line is eq. (2).

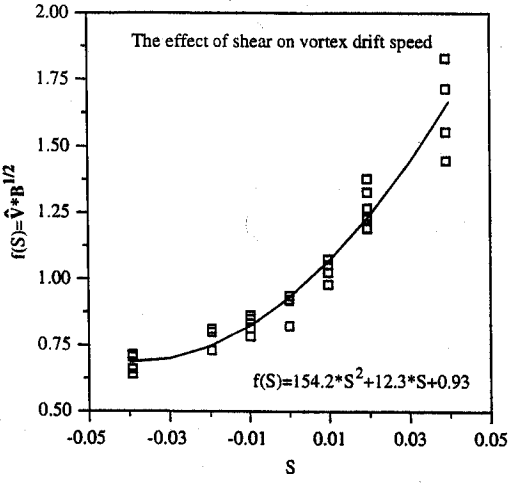

Fig. 6. The effect of meridional shear is seen by plotting $f = \hat{V}B^{+1/2}$ against S, as defined in eq. (16). The least squares quadratic fit (17) is shown with a solid line.

Figs. 5 and 6 and eq. (17) show that meridional shear increases the speed of beta drift when the shear vorticity has the opposite sign to the primary vortex vorticity. The drift speed is reduced when the two vorticities have the same sign. The strong curvature in Fig. 6 indicates that the magnitude of the meridional shear effect is much larger in the opposite sign case, as noted by Williams and Chan (1994).

Data from these 30 simulations suggests that the angle of beta drift is independent of B, as it was in Section 2. The drift angle increases slightly with shear. The relationship $\theta_d(S)$ with $b=1$ can be approximated by

$$\theta_d(S) = 325° + 200° S. \qquad (18)$$

This increase has a simple geometric interpretation. The increase of the drift angle with shear is due to a clockwise shift in the position of beta-gyres caused by the shearing advection by the background flow. The clockwise rotation in the gyre position causes the vortex to be advected in a more northward direction.

We have made no attempt to extend our results to include an east-west variation in meridional wind (i.e., $V(x)$). The specification of such an environment would lead to large scale vorticity tendencies in the beta-plane formulation (see equation 1) making the vortex drift more difficult to define.

Our study of the dU/dy effect in this section, while neglecting the other components of the deformation (i.e., dU/dx, dV/dx, dV/dy), may be problematic. To investigate this issue, we computed statistics for all four components of the horizontal windfield deformation at 2 points in the subtropics; one in the western north Pacific and one in the western north Atlantic (20°N 140°E

and 20°N 55°W). As we wished to sample the shears associated with the large scale environment, rather than the hurricanes themselves, we examined the month of June, just before hurricanes begin. The shear values were computed using a 5° centered difference in the NCEP/NCAR Reanalysis dataset.

According to Table 2, only the dU/dy term has a mean value which approaches a magnitude of 1×10^{-5} s^{-1}, although in the Atlantic at 700 mb in 1995, it's mean value happens to be much smaller. The positive mean values for dU/dy indicate that our test points lie in the vicinity of the subtropical ridge. The standard deviations (i.e., sigma values) are also significant as they represent the range of day-to-day environmental shear values that the test point experiences. Generally, the standard deviations for dU/dy are about $2\times$ that of dV/dx, while for the other components (dU/dx and dV/dy) the standard deviations are smaller still. This data provides some support for our emphasis on the effect of dU/dy on beta drift.

5. A general empirical drift law

In Section 2, we showed that for $S=0$ and variable b, the drift speeds satisfy the square root B scaling and the drift angles are independent of B. In Section 3, we showed that the same result applies for $b=1$ and variable S. To proceed, we now assume that these results apply to the entire (b,S) parameter space. Thus

$$\hat{V}=C(b,S)B^{-1/2} \tag{19}$$

for the drift speed, while the drift direction must be of the form

$$\theta_d=D(b,S). \tag{20}$$

The function $C(S,b)$ should approximate (11) and (17) and the function $D(S,b)$ should approximate (13) and (18) but these constraints are not sufficient to determine these functions. For this purpose, we have carried out 35 additional simulations using seven values of shear (S) and 5 vortex profiles b. As the dependence on B is already established, the parameter B is fixed at $B=0.00715$ for these runs. The results are given in Table 3. The reader should be aware that the values in Table 3 contain random errors due to transient track oscillations. In spite of these errors, clear trends are evident in Table 3. The scaled drift speeds increase with increasing positive shear S and with decreasing profile exponent b. The drift directions exhibit a rather complex dependence on b and S. For $b=1.33$, θ_d is not very sensitive to shear. As b decreases (i.e., wider vortex profiles), θ_d becomes much more sensitive to shear. Generally, positive shear gives greater drift angles. In the extreme case of $b=0.33$, strong negative shear gives a WNW drift direction ($\theta_d=293°$)

Table 2. *Shear value statistics, June 1995*

	dU/dx	$dU/dy(=\alpha)$	dV/dx	dV/dy
Pacific 850 mb				
mean	−0.15	1.06	−0.12	0.17
sigma	0.38	0.77	0.42	0.35
Pacific 700 mb				
mean	−0.14	0.81	−0.09	0.18
sigma	0.41	1.1	0.52	0.41
Atlantic 850 mb				
mean	0.03	0.62	−0.01	0.01
sigma	0.29	0.56	0.38	0.31
Atlantic 700 mb				
mean	0.23	0.07	0.10	−0.27
sigma	0.36	0.96	0.50	0.38

Pacific point at 20°N, 140°E. Atlantic point at 20°N, 55°W. All units ($\times 10^5$ s^{-1}).

Table 3. *Drift speed (scaled) and direction for various profile exponents and meridional shear*

	$\hat{V}B^{1/2}$				
S/b	1.33	1.0	0.66	0.5	0.33
−0.04	0.48	0.52	0.64	0.84	0.69
−0.02	0.58	0.64	0.82	0.83	0.70
−0.01	0.68	0.77	0.91	1.18	0.93
0.00	0.68	0.89	0.90	1.39	1.61
0.01	0.82	0.99	1.44	1.51	1.95
0.02	1.09	1.21	1.89	1.82	2.42
0.04	1.40	1.72	1.88	1.89	2.33
	θ_d (degrees from north)				
S/b	1.33	1.0	0.66	0.5	0.33
−0.04	314	308	302	301	293
−0.02	325	314	308	303	290
−0.01	326	320	314	300	286
0.00	334	326	321	312	313
0.01	329	325	329	317	331
0.02	327	325	330	328	328
0.04	324	333	340	344	341

while strong positive shear gives a NNW direction ($\theta_d = 341°$). This trend is consistent with the idea that meridional shear rotates the steady state positions of the beta gyres.

Because of the random errors in the drift results shown in Table 3, it is unclear how detailed a curve fitting procedure we should undertake. The major trends in the drift speed are approximately represented by the function

$$C(b,S) = b^{-(0.67-8|S|)}\,(154S^2 + 12S + 0.9), \tag{21}$$

which reduces to (11) and (17).

The major trends in the drift angle data can be approximately represented by a bilinear function

$$D(b,S) = 310° + 15°b + 600(1.33-b)S. \tag{22}$$

Except for the larger values of b, which are probably not relevant for real hurricanes, the formula (22) fits the data within $\pm 5°$. This error in fitting is about the same as the scatter in the data itself. Note that (22) does not reduce exactly to (13).

Eqs. (19–22) comprise an empirical drift law for hurricanes. The dimensional eastward and northward components of the drift vector can be computed from:

$$V_{d_x} = C(b,S) r_m \sqrt{V_m \beta}\, \sin\,(D(b,S)), \tag{23}$$

$$V_{d_y} = C(b,S) r_m \sqrt{V_m \beta}\, \cos\,(D(b,S)). \tag{24}$$

The total hurricane motion vector is the sum of the drift vector V_d and the environmental steering vector V_E:

$$V_x = V_{d_x} + V_{E_x}, \tag{25}$$

$$V_y = V_{d_y} + V_{E_y}. \tag{26}$$

The parameters influencing hurricane motion, particularly α, β and V_E, would generally change with time requiring that (21–26) be reevaluated at each time step.

To illustrate the influence of the vortex profile and the meridional shear on hurricane tracks, we consider a simple prototype problem of constant meridional shear ($\alpha = 1.175 \times 10^{-5}$ s^{-1}) near the "subtropical ridge", i.e. the latitude of zero zonal wind, in the northern hemisphere. The environmental wind field is assumed to be purely zonal and independent of longitude and time. In this problem, by neglecting changes in beta with latitude, the drift velocity is constant in time. We imagine two hurricanes, each with radius $r_m =$ 100 km and maximum wind speed $V_m = 30$ m/s. Hurricane A has $b = 1$ and hurricane B has a more realistic vortex profile with $b = 0.4$. The nondimensional shear parameter for both hurricanes is $S = 0.04$.

4 cases are shown in Fig. 7. The tracks of both hurricanes are computed with and without the influence of shear on the drift velocity. Thus, in the case labelled "no shear" (NS), S is set equal to zero in (21, 22) while in the shearing case S, the actual value of $S = 0.04$ is used. The drift velocity components (V_{d_x}, V_{d_y}) from (23, 24) for cases ANS, BNS, AS and BS are (−0.89, 1.27), (−2.0, 2.1), (−1.28, 2.5) and (−1.43, 3.61) in units of meters per second. Using (14, 25–26), the tracks are perfect parabolas given parametrically by

$$x(t) = (\alpha y_0 + V_{d_x})t + \left(\frac{1}{2}\alpha V_{d_y}\right)t^2 + x_0, \tag{27}$$

$$y(t) = V_{d_y} t + y_0, \tag{28}$$

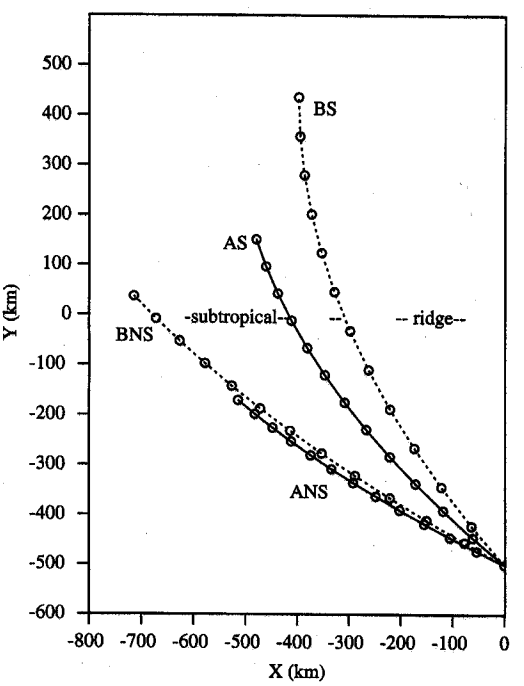

Fig. 7. The influence of the vortex profile and meridional shear on hurricane tracks near the subtropical ridge. Hurricanes A and B have different vortex exponents (i.e., $b = 1.0$ and 0.4 respectively). The symbols S and NS indicate whether or not the influence of environmental shear on the drift velocity is included in the calculation. The location of the vortex is shown at six hour intervals. The vortex is followed for 72 h.

where x_0 and y_0 describe the initial position of the hurricane. The tracks for $x_0=0$ and $y_0=-500$ km are shown in Fig. 7. (The idea that a hurricane track might take the form of a parabola goes back to a qualitative comment of Loomis (1868, page 148).)

With the shear effect neglected, hurricanes A and B exhibit similar drift directions but hurricane B, with its smaller exponent, moves more rapidly. The effect of shear is primarily to increase the northward component of drift. In case BS (i.e., hurricane B with shear), the hurricane moves quickly to the north and feels the influence of the environmental westerlies, north of the subtropical ridge.

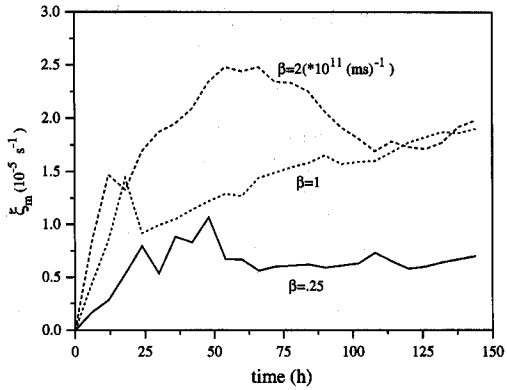

Fig. 8. The maximum beta gyre vorticity ξ_m in units $s^{-1} \times 10^5$ is plotted against time (h). Three numerical simulations with $b=1$ and with different values of beta are shown ($\beta=0.25$, 1, 2×10^{-11} m^{-1} s^{-1}). A crude steady state is reached after about 40 h.

6. Discussion

The fact that the approximate proportionality $V_d \sim \sqrt{\beta}$ in (19) is retained in the presence of shear, and for various vortex profiles, suggests a robustness to this relationship. It may signify a simple, but as yet undiscovered, underlying mathematical structure to the beta drift problem. At first sight, this square-root relationship seems surprising as we might expect the strength of the beta-gyre vorticity ξ to be proportional to beta, (i.e., $\xi \sim \beta$). If this were true, and if the drift velocity V_d were proportional to ξ (i.e., $V_d \sim \xi$), then a linear proportionality $V_d \sim \xi \sim \beta$ would follow. To explain the square-root relationship in (19), one or both of these proportionalities (i.e., $\xi \sim \beta$ and $V_d \sim \xi$) must be incorrect.

To determine the relationship between gyre vorticity and beta, we performed eleven runs with different values of beta. In these runs, $b=1$, $\alpha=0$, $r_m=100$ km, $V_m=30$ m/s while beta varied by a factor of 12, from 0.25 to 3.0×10^{-11} m^{-1} s^{-1}. At 6-h intervals, during the steady portion each run, the vortex velocity field was mapped to cylindrical coordinates centered on the vortex and the wavenumber-one gyre vorticity pattern was determined as a function of radius. The maximum value of the gyre vorticity ξ_m was recorded. This maximum value always occurred at a radius approximately equal to 5 r_m. Fig. 8 shows the evolution of ξ_m for 3 of the 11 runs. As noted before, the quality of the steady state is imperfect. By sampling at several times, a reasonable averaged value can be obtained. These values are plotted against beta in Fig. 9.

As shown in Fig. 9, the non-dimensional maximum gyre vorticity $\hat{\xi}_m=\xi_m r_m/V_m$ increases with the non-dimensional beta B. On a log-log plot, the best fit line has a slope of 0.63.

$$\hat{\xi}_m = 1.74\, B^{0.63}, \qquad (29)$$

valid for $b=1$, $\alpha=0$ and B between 0.00084 and 0.01. The rather scattered data can also be fit

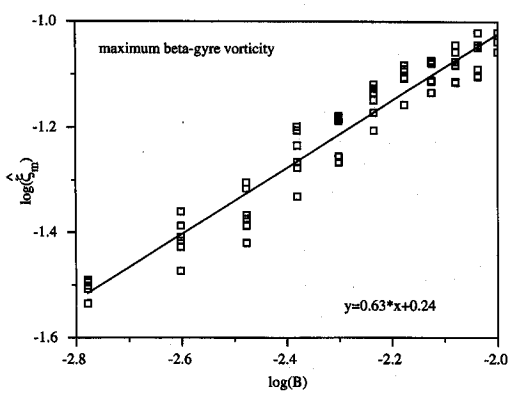

Fig. 9. The non-dimensional maximum beta gyre vorticity $\hat{\xi}_m$ is plotted against the non-dimensional beta parameter. Several points from each of eleven simulations are shown. A log–log plot is used to reveal power law relationships. The solid line is eq. (29).

reasonably well by an equivalent formula with an exponent of $\frac{1}{2}$.

$$\hat{\xi}_m = 0.85\ B^{1/2}. \tag{30}$$

The data does not support a direct proportionality between beta and ξ_m (i.e., $\hat{\xi}_m \sim B$).

The second possibility mentioned above is that the proportionality $V_d \sim \zeta_m$ might be incorrect. This possibility can be excluded by noting that the pattern of gyre vorticity and stream function appeared to be nearly independent of beta in our runs. For example, the radius of maximum vorticity did not change significantly with beta. Under this condition, the drift velocity could only be proportional to the magnitude of the gyre vorticity. Furthermore, it is a particular property of wavenumber-one vorticity that the induced velocity at the origin is independent of the radius at which the vorticity containing ring is located (Ross & Kurihara, 1993). Thus, even if the gyre vorticity did shift to larger or smaller radius, the drift velocity would not be affected. We conclude that the root beta scaling for drift velocity (19) arises from (30), giving the dimensional proportionality $V_d \sim \xi \sim \sqrt{\beta}$.

How can the relationship $\xi \sim \sqrt{\beta}$ be explained? One possibility is that a feedback process operates in which an increased drift velocity weakens the beta gyres. To understand this possibility we note that according to (1), beta-gyre vorticity is rotated by the vortex winds from the NE-SW positions to the NW-SE positions where it is destroyed by the north-westward drift of the vortex. Thus, the steady-state beta-gyre strength ξ may be maintained as a balance between β and V_d. We speculate that this balance could lead to the relationship $\xi \sim \beta/V_d$. Then, using $V_d \sim \xi$ we have $V_d \sim \beta/V_d$ or $V_d \sim \sqrt{\beta}$, in agreement with (19).

If the rotation of the beta gyres into the cyclone's path is an important factor in determining the beta-gyre strength, then the effect of meridional shear on drift speed (see Section 4) might be understood as follows. The meridionally sheared zonal wind does not advect planetary vorticity to create beta-gyres, but it does influence the rate at which the beta-gyre vorticity is rotated into the path of the drifting vortex, and thus destroyed. Positive meridional shear works against the beta-gyre vorticity advection by the primary vortex and thus allows the beta-gyres to become more intense; and the drift more rapid. Negative meridional shear assists in the rotation of the beta-gyres into the path of the drifting vortex and thus weakens the gyres and slows the drift. According to this argument, the factor $f(S)$ in (17) describes the influence of shear on the steady-state strength of the beta-gyre. Such an explanation, if correct, would complement the kinetic energy analysis by Wang and Li (1995).

7. Application to ensemble forecasting

The practical application of the current result (19–26) is fundamentally limited by uncertainty in whether ideal barotropic dynamics (i.e., eq. (1)) captures the essential elements of hurricane drift. This issue has been widely discussed in the literature (e.g., DeMaria 1985). Other mechanisms such as asymmetric friction, convection or winds aloft could also induce a drift relative to the mean advective velocity. The advantage of steady-state beta gyre theory, if there is one, is that it is simple and easy to parameterize. It should be thoroughly tested against real data before it is used.

One practical application of an empirical drift law is in the ensemble forecasting of hurricane tracks. The goal of ensemble forecasting is to determine the range of possible future tracks and their respective probabilities. We envision a procedure similar to the beta-advection-model (BAM) described by Marks (1992) and DeMaria et al. (1992). The space-time output of a global or regional numerical forecast model is used to obtain the advecting velocity and the meridional shear along a potential hurricane track. Satellites or research aircraft are used to determine the initial hurricane position, strength and wind profile. With these inputs, the empirical drift law can be integrated in time to forecast the hurricane track. Because each of the inputs to the model is uncertain, the drift law integration can be repeated many times to include a range of possible input data. The number of required integrations can be estimated as follows. The US National Center for Environmental Prediction is currently doing ensemble forecasts with about 40 forecast runs (Toth and Kalnay, 1993; Tracton and Kalnay, 1993). From each run, both shallow and deep advecting wind averages can be derived, (Veldon and Leslie, 1991). The choice of vortex parameters r_m, V_m and b are also uncertain with perhaps 2

reasonable choices for each. The combination of these choices require $40\times2\times2\times2\times2=640$ drift integrations. Using a drift law, these 640 runs could be done faster than one run using a nested grid barotropic model. In some cases, the predicted tracks will cluster tightly giving extra confidence to the forecast while in other cases the predicted tracks will diverge strongly. Only by using a closed form drift law, can hundreds of track integrations be carried forward in the short time allowed for the generation of a useful forecast.

8. Conclusions

We have shown that a steady state formulation of dimensional analysis successfully collapses the results from a variety of numerical beta drift calculations, including those of previous investigators. This success adds support to the concept of steady state drift and to the numerical methods used to simulate it.

When the effect of beta is sufficiently small, specifically when $B<0.01$, vortex beta drift speed and direction are governed by the formulae:

$$\hat{V}=C(b,S)B^{-1/2},$$

$$\theta_d=D(b,S),$$

over a wide range of vortex profiles b and environmental shear S. The functions C and D have been determined empirically from a large number of numerical simulations.

These formulae imply that $V_d\sim\sqrt{\beta}$ and that θ_d is independent of beta over a wide range of conditions. The proportionality $V_d\sim\sqrt{\beta}$ occurs because the beta gyre vorticity is approximately proportional to the square root of beta, i.e., $\xi\sim\sqrt{\beta}$.

Our analysis of 35 numerical simulations indicates that $C(b,S)$ and $D(b,S)$ have the following properties. The broader vortex profiles have a faster drift speed and more sensitivity to environmental shear. Increasing environmental shear increases the speed and the angle of beta drift, presumably by modifying the vorticity balance which maintains the beta gyres.

To the extent that hurricane drift is governed by simple barotropic vorticity dynamics, the empirical drift law derived herein (19–22) may allow massive ensemble forecasting of hurricane tracks. In this way, the uncertainty in the large scale prediction of steering winds as well as uncertainties in the hurricane size, strength and profile may be accounted for.

The current results for beta-drift might be applicable to other vortex drift problems that have an asymmetry analogous to the beta term in (1). One example is the situation where the environmental flow has a horizontally non uniform relative vorticity $\xi_e(x)$, as discussed by Smith and Ulrich (1993) and Williams and Chan (1994). In this case, the gradient $\nabla\xi_e$ may act like a "pseudo-beta". It is convenient to define a beta-vector $\overline{\beta}=\nabla(\xi_e+f)$ pointing toward "pseudo-north". The drift angle computed from (20, 22) should be measured clockwise from pseudo-north. If desired, the effect of environmental shear can be included by defining "α" as the derivative of the pseudo-eastward flow in the pseudo-north direction. Williams and Chan (1994) find that the analogy with beta breaks down with strong shear.

Shallow flows in a rotating coordinate system with a sloping bottom boundary also experience a pseudo-beta effect. Examples include ocean vorticies over the coastal slopes (Smith and O'Brien, 1983) and hurricanes moving ashore over gentle sloping topography. In this case, the beta-vector could be defined as $\overline{\beta}=H\nabla(f/H)$. This beta-vector points toward shallower fluid depths. The "meridional shear" (α) is the shear in the "along-shore" environmental current. The resulting "northwestward" drift, given by (19–22), moves the vortex upslope and leftward.

9. Acknowledgements

The comments of Mark De Maria and Lloyd Shapiro and five anonymous reviewers are appreciated. This research was supported by the National Science Foundation Grant ATM-8914138 and the Department of the Navy, Office of Naval Research Grant N00014-93-1-0238 to Yale University, and by the Office of Naval Research Grant N00014-90-J-1383 to the University of Hawaii.

REFERENCES

Chan, J.C-L and Williams, R. T. 1989. Analytical and numerical studies of the beta effect in tropical cyclonic motion. *J. Atmos. Sci.* **44**, 1257–1265.

DeMaria, M. 1985. Tropical cyclone motion in a non-divergent barotropic model. *Mon. Wea. Rev.* **113**, 1199–1210.

DeMaria, M., Aberson, S. D., Oyama, K. V. and Lord, S. J. 1992. A nested spectral model for hurricane track forecasting. *Mon. Wea. Rev.* **120**, 1628–1643.

Grimshaw, R., Tang, Y. and Broutman, D. 1994. The effect of vortex stretching on the evolution of barotropic eddies over a topographic slope. *Geophys. Astrophys. Fluid Dynamics* **76**, 43–71.

Loomis, E. 1868. *A treatise on meteorology*. New York: Harper and Brothers, 300 p.

Marks, D. G. 1992. *The beta and advection model for hurricane track forecasting*. NOAA Tec. Memo. NWS-NMC-70, National Meteorological Center, Camp Springs, MD, 89 p.

Ross, R. J. and Kurihara, Y. 1992. A simplified scheme to simulate asymmetries due to the beta effect in barotropic vorticies. *J. Atmos. Sci.* **49**, 1620–1628.

Smith, R. B. 1993. A hurricane beta-drift law. *J. Atmos. Sci.* **50**, 3213–3215.

Smith, I. V., D. C. and O'Brien, J. J. 1983. The interaction of a two-layer mesoscale with bottom topography. *J. Phys. Ocean.* **13**, 1681–1697.

Smith, R. K. and Ulrich, W. 1993. Vortex motion in relation to the absolute vorticity gradient of the vortex environment. *Quart. J. Roy. Met. Soc.* **199**, 207–215.

Toth, Z. and Kalnay, E. 1993. Ensemble forecasting at NMC. The generation of perturbations. *Bull. Amer. Meteor. Soc.* **74**, 2317–2330.

Tracton, M. S. and Kalnay, E. 1993. Operational ensemble prediction at the National Meteorological Center: Practical aspects. *Wea. Forecasting* **8**, 379–398.

Veldon, C. S. and Leslie, L. M. 1991. The basic relationship between tropical cyclone intensity and the depth of the environmental steering layer. *Wea. Forecasting* **6**, 244–253.

Williams, R. T. and Chan, J. C-L. 1994. Numerical studies of the beta effect in tropical cyclone motion. Part II: Zonal mean flow effects. *J. Atmos. Sci.* **51**, 1065–1076.

Wang, B. and Li, X. 1992. The beta drift of three-dimensional vortices. A numerical study. *Mon. Wea. Rev.* **120**, 579–593.

Wang, B. and Li, X. 1995. Propagation of a tropical cyclone in a meridionally varying zonal flow. An energetics analysis. *J. Atmos. Sci.* **52**, 1421–1433.